Hilbert Transform Based Approach to Improve Extraction of "Drive-by" Bridge Frequency

Chengjun Tan*1, Nasim Uddin²

^{*1} Graduate Research Assistant/Ph.D. Candidate
Civil & Environmental Engineering Department, The University of Alabama at Birmingham, 1075 13th St S,
Birmingham, AL 35205 USA

²Chief Editor for ASCE Journal of Natural Hazards Review/ Professor
Civil & Environmental Engineering Department, The University of Alabama at Birmingham, 1075 13th St S,
Birmingham, AL 35205 USA

(Received, Revised, Accepted)

Abstract. Recently, the concept of "drive-by" bridge monitoring system using indirect measurements from a passing vehicle to extract key parameters of a bridge has been rapidly developed. As one of the most key parameters of a bridge, the natural frequency has been successfully extracted theoretically and in practice using indirect measurements. The frequency of bridge is generally calculated applying Fast Fourier Transform (FFT) directly. However, it has been demonstrated that with the increase in vehicle velocity, the estimated frequency resolution of FFT will be very low causing a great extracted error. Moreover, because of the low frequency resolution, it is hard to detect the frequency drop caused by any damages or degradation of the bridge structural integrity. This paper will introduce a new technique of bridge frequency extraction based on Hilbert Transform (HT) that is not restricted to frequency resolution and can, therefore, improve identification accuracy and detect bridge damages represented as changing the fundamental frequency of the bridge. In this paper, deriving from the vehicle response, the closed-form solution associated with bridge frequency removing the effect of vehicle velocity is discussed in the analytical study. Then a numerical Vehicle-Bridge Interaction (VBI) model with a quarter car model is adopted to demonstrate the proposed approach. Finally, this proposed approach is applied to detect the bridge frequency drop caused by the structural damage so as to estimate the bridge condition.

Keywords: Hilbert Transform, bridge frequency, drive-by bridge inspection, bridge health monitoring, non-destructive evaluation;

1. Introduction

Bridge structures are the intrinsic components of transportation infrastructure network. Nowadays these structures are increasingly subject to degradation due to aging, environment and overload. Periodic monitoring of bridge is, therefore essential to maintain strategy since it can provide early warning if the inspected bridge becomes unsafe. Traditionally, bridge maintenance has mostly relied to visual inspection approaches which are highly dependent on staff member experience and subjective determine. These approaches can only detect bridge damage when it is visible. A number of bridges collapsed catastrophically such as I-35W Mississippi River bridge, whereas, they had been visually inspected just before the disaster. Thus, Chupanit and Phromsorn

*Chengjun Tan, Ph.D. Student E-mail: tan1990@uab.edu

-

(2012) have suggested that the visual inspection alone may not be sufficient to assess the bridge health condition.

The last decades, the bridge structural health monitoring (SHM) has developed dramatically which rely on the automatic detection of anomalous structural behavior. One of the most popular SHM approaches assess bridge condition via extracting dynamic properties of the bridge such as natural frequency, damping ratio, and mode shapes from dynamic response of structures for non-destructive damage assessment (Carden 2004, Malekjafarian, McGetrick et al. 2015). In these SHM systems using vibration data from the structure are referred to as the direct approach, which requires a larger number of sensors installed on bridge structures (Carden 2004). These SHM techniques have following drawbacks: expensive, time-consuming and even dangerous (Malekjafarian, McGetrick et al. 2015). From another perspective, the implementation of SHM for short and medium span bridges is not widespread, which represent a large portion of the bridge inventory of the road network (Malekjafarian, McGetrick et al. 2015). Therefore, there is a necessity to find a less expensive SHM method that can be applied to a wide range of bridges.

Recently, the indirect approach or what has been known as 'drive-by bridge inspection' is becoming an intriguing topic in the application of bridge SHM technique. This indirect approach extracts bridge dynamic properties from dynamic response of a passing vehicle over the bridge, which is first proposed by Yang and Lin (2005), Yang and Chang (2009). The authors derived a closed-form solution of vehicle response, where a vehicle is modeled as a sprung mass and a bridge as a simple support beam. It has shown that the vehicle response contains the vibration components dominated by the natural frequency of bridge, and that has been demonstrated by the numerical simulation with VBI model. The feasibility of extracting natural frequency of bridge from a passing vehicle in practice has been experimentally verified by Lin and Yang (2005), Yang and Chang (2009).

Following the idea of the indirect approach, González, Obrien et al. (2012), Keenahan, Obrien et al. (2013) have theoretically investigated the method of extracting related bridge damping from vehicle history. González, Obrien et al. (2012) have pointed out that the damping value of bridge can be calculated by the minimum road profile estimation error from two axles with a half car model. Keenahan, Obrien et al. (2013) have presented that the damping change in the bridge can be detected when the axle accelerations of the trailer are subtracted from one another. They pointed out that this method is more effective for monitoring damping in short bridges.

On the other hand, a number of methods for constructing mode shape of the bridge based on such indirect approach have been proposed (Zhang, Wang et al. 2012, Malekjafarian and Obrien 2014, Oshima, Yamamoto et al. 2014, Yang, Li et al. 2014, Obrien and Malekjafarian 2016, Malekjafarian and Obrien 2017). Yang, Li et al. (2014) theoretically constructed bridge modal shape from a passing vehicle over the bridge through applying HT combined with band-pass filter technique. They pointed out that such indirect measurements from the instrumented vehicle can provide a better screening for the bridge degrees of freedom (DOF) than the direct measurements from a sensor mounted on the bridge structure. Zhang, Wang et al. (2012) have developed a simple approach to approximately extract bridge mode shape squares from the passing vehicle response and proposed a new damage index based on this extraction of mode shape, which is more sensitive to structural damage. The validity of this proposed method has been demonstrated by numerical simulations and simple experiments in the lab.

Furthermore, signal processing tool such as wavelet transform and HT are increasingly applied on the "drive by" bridge SHM (Cunha, Caetano et al., Yang and Chang 2009, Nguyen and Tran 2010, Hester and González 2012, Khorram, Bakhtiari-Nejad et al. 2012, McGetrick and Kim 2013, Mahato, Teja et al. 2017, Obrien, Malekjafarian et al. 2017, Tan, Elhattab et al. 2017, Tan, Elhattab et al. 2017). On account of their high sensitivity for discontinuity of signal, they are mostly used to localize the structural damage location. In addition, HT can assist to extract higher mode frequency or modal shape of the bridge from the vehicle response.

The natural frequency of bridges as one of the most basic vibration parameters reflecting bridges dynamic characteristic, it was constantly referred as a damage index to estimate bridge condition. In the application of tradition bridge SHM, a published review paper (Carden 2004) have shown that there were 65 publications working on the detection of structural damage through frequency drops. However, rarely studies were focused on this point in the application of "drive-by" bridge SHM. One of the main reasons is that the higher vehicle velocity leads to short data of vehicle responses, resulting in low frequency resolution when applied with FFT. Consequently, the identification accuracy of bridge frequency is poor. Tan, Elhattab et al. (2017) have developed a wavelet-based approach to identify bridge frequency without restricting to frequency resolution and can be used to detect the frequency drop caused by structural damage. However, it has shown that with the increase in vehicle velocity, the identification accuracy will decrease either. Studies have pointed out that the higher vehicle velocity has a strong negative influence on the recognition of bridge frequency in "drive-by" bridge SHM.

This paper will introduce a new bridge frequency extracting approach from a passing vehicle based on HT combined with band-pass filter technique. At first, in order to highlight the dynamic VBI response, a closed-form solution of vehicle response is adopted in the analytical study. In this regard, the bridge is modeled as a simply supported beam and vehicle as a sprung mass. Deriving this closed-form solution with HT combined with the band-pass filter, formulation representing the bridge frequency is divided. In addition, the vehicle velocity parameter is investigated and it can be removed from this formulation to improve identification accuracy. Then, a numerical VBI model with a quarter car model is adopted to demonstrate the proposed approach. Finally, this proposed approach is applied to detect the bridge frequency drop caused by the structural damage so as to estimate the bridge condition.

2 Hilbert Transform

In this section, a brief introduction of HT is presented. Mathematically, given a real-valued

mono-component function of
$$s(t)$$
, the Hilbert transform of $s(t)$ is defined as (Huang 2014):
$$\hat{s}(t) = H(s(t)) = \frac{1}{\pi} PV \int_{-\infty}^{+\infty} \frac{s(\tau)}{t - \tau} d\tau \tag{1}$$

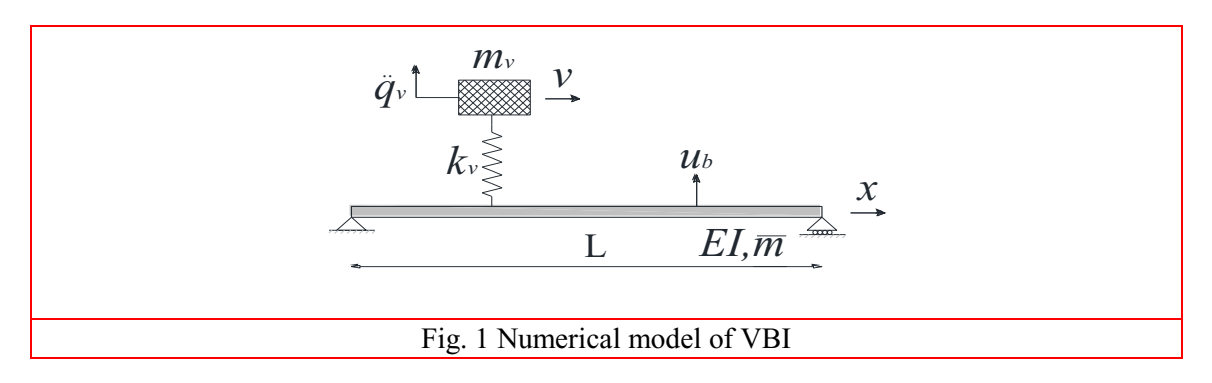
where PV denotes the Cauchy principal value. Practically, it defines the HT as the convolution of s(t) with the kernel function $1/\pi t$. Therefore, $\hat{s}(t)$ is referred as the orthogonal projection of s(t). Using these two orthogonal component, the analytic signal z(t) can be constructed in the form

$$z(t) = s(t) + i\hat{s}(t) = A(t)e^{i\theta(t)}$$
(2)

where
$$A(t) = \sqrt{s^2(t) + \hat{s}^2(t)}, \, \theta(t) = \arctan\left(\frac{\hat{s}(t)}{s(t)}\right) \tag{3,4}$$

In above equation, the time-dependent functions of A(t) and $\theta(t)$ are the instantaneous amplitude function and instantaneous phase function, respectively, of the original function s(t). Using vector representations in complex plane, A(t) and $\theta(t)$ can be obtained easily.

3. Formulation of the analytical theory



In order to highlight the major dynamic characteristics of the coupled VBI system, a simplified numerical model will be adopted, as given in Fig. 1. The vehicle is simply simulated as a lumped mass m_v , supported by a spring of stiffness k_v and passing with constant speed v across a simply supported beam of length v. This beam is assumed to be of the Bernoulli–Euler type with constant cross section and ideal smooth pavement. Through neglecting the damping effects of both bridge and vehicle, the equations of motion for the bridge and vehicle can be written as follows:

$$\overline{m}\ddot{u} + EIu^{""} = f_c(t)\delta(x - vt)$$

$$m_v \ddot{u} + k_v(q_v - u|_{x=vt}) = 0$$
(5)
(6)

where \overline{m} denotes the bridge mass per unit length, E young elastic modulus, I moment of inertia, u(x,t) vertical displacement of beam, and $q_v(t)$ vertical displacement of the vehicle, measured from the static equilibrium position, and a dot and a prime represent the derivative with relative to time t and longitudinal coordinate x of the beam, respectively. The contact force between beam and vehicle $f_c(t)$ can be expressed as

$$f_c(t) = -m_v g + k_v (q_v - u|_{x=vt})$$
(7)

where g represents the gravitational acceleration.

Using the modal superposition method, the solution of the bridge displacement response u(x,t) in equation (5) can be expressed in term of modal shapes $\sin(n\pi x/L)$ and generalized coordinates $q_{b,n}(t)$,

$$u(x,t) = \sum_{n=1}^{\infty} \sin \frac{n\pi x}{L} q_{b,n}(t)$$
 (8)

Accordingly, one can obtain the solution of the displacement of the test vehicle in equation (6) as following (Yang and Lin 2005, Yang and Chang 2009, Yang, Li et al. 2014)

$$q_{v}(t) = \sum_{n=1}^{\infty} \left\{ A_{1,n} \cos\left(\frac{(n-1)\pi v}{L}\right) t + A_{2,n} \cos\left(\frac{(n+1)\pi v}{L}\right) t + A_{3,n} \cos(\omega_{v}t) + A_{4,n} \cos\left(\omega_{b,n} - \frac{n\pi v}{L}\right) t + A_{5,n} \cos\left(\omega_{b,n} + \frac{n\pi v}{L}\right) t \right\}$$

$$(9)$$

where the coefficient of $A_{4,n}$ and $A_{5,n}$ are

$$A_{4,n} = \frac{-S_n \Delta_{st,n} \omega_v^2}{2(1 - S_n^2) \left(\omega_v - \omega_{b,n} + \frac{n\pi v}{L}\right) \left(\omega_v + \omega_{b,n} - \frac{n\pi v}{L}\right)}$$

$$A_{5,n} = \frac{S_n \Delta_{st,n} \omega_v^2}{2(1 - S_n^2) (\omega_v + \omega_{b,n} + \frac{n\pi v}{L}) (\omega_v - \omega_{b,n} - \frac{n\pi v}{L})}$$
and the bridge frequency $\omega_{b,n}$, vehicle frequency ω_v , velocity parameter S_n , and vehicle-induced

static deflection $\Delta_{st,n}$ of the beam, of the n-th mode are defined as

$$\omega_{b,n} = \left(\frac{\pi v}{L}\right)^2 \sqrt{\frac{EI}{m}}$$

$$\omega_v = \sqrt{\frac{k_v}{m_v}}$$

$$S_n = \frac{n\pi v}{L\omega_{b,n}}$$

$$\Delta_{st,n} = \frac{-2\omega_v g L^3}{n^4 \pi^4 EI}$$

$$(12,13,14,15)$$

Similar to the coefficient of $A_{4,n}$ and $A_{5,n}$ in equation (10, 11), $A_{1,n}$ $A_{2,n}$ and $A_{3,n}$ are time irrelevant coefficients determined by parameters of ω_v , $\omega_{b,n}$, $\Delta_{st,n}$ and S_n . However, it won't be presented herein since it is not of concern in this study.

Therefore, taking twice derivative of the vehicle displacement response, one can obtain the vehicle acceleration response

$$\ddot{q}_{v}(t) = \sum_{n=1}^{\infty} \left\{ \bar{A}_{1,n} \cos\left(\frac{(n-1)\pi v}{L}\right) t + \bar{A}_{2,n} \cos\left(\frac{(n+1)\pi v}{L}\right) t + \bar{A}_{3,n} \cos(\omega_{v}t) + \bar{A}_{4,n} \cos\left(\omega_{b,n} - \frac{n\pi v}{L}\right) t + \bar{A}_{5,n} \cos\left(\omega_{b,n} + \frac{n\pi v}{L}\right) t \right\}$$

$$(16)$$

with the coefficients of
$$\bar{A}_{4,n}$$
 and $\bar{A}_{5,n}$ as
$$\bar{A}_{4,n} = \frac{S_n \Delta_{st,n} \omega_v^2}{2(1 - S_n^2)(\omega_v - \omega_{b,n} + \frac{n\pi v}{L})(\omega_v + \omega_{b,n} - \frac{n\pi v}{L})} (\omega_{b,n} - \frac{n\pi v}{L})^2$$

$$\bar{A}_{5,n} = \frac{-S_n \Delta_{st,n} \omega_v^2}{2(1 - S_n^2)(\omega_v + \omega_{b,n} + \frac{n\pi v}{L})(\omega_v - \omega_{b,n} - \frac{n\pi v}{L})} (\omega_{b,n} + \frac{n\pi v}{L})^2$$
(17,18)

Apparently, the vehicle acceleration response of equation (16) is dominated by five frequencies, i.e., two shifted driving frequencies $(n-1)\pi v/L$ and $(n+1)\pi v/L$, vehicle frequency ω_v , and two shifted bridge frequencies $\omega_{b,n} - n\pi v/L$ and $\omega_{b,n} + n\pi v/L$.

To extract the frequency of bridge from the vehicle acceleration response with this proposed HT approach, the component response corresponding to the bridge frequency of n-th mode should be singled out via an appropriate filtering technique. According to equation (16), the extracted component response R_b associated with single frequency of bridge (n-th mode) is (Yang, Li et al. 2014)

$$R_b(t) = \bar{\bar{A}}_{4,n} \cos\left(\omega_{b,n} - \frac{n\pi v}{L}\right) t + \bar{\bar{A}}_{5,n} \cos\left(\omega_{b,n} + \frac{n\pi v}{L}\right) t \tag{19}$$

The filtering signal of R_b is a narrow-band time series and thus can be applied with HT to produce its transform pair,

$$\hat{R}_b(t) = H[(R_b(t))] = \bar{\bar{A}}_{4,n} \sin\left(\omega_{b,n} - \frac{n\pi v}{L}\right) t + \bar{\bar{A}}_{5,n} \sin\left(\omega_{b,n} + \frac{n\pi v}{L}\right) t \tag{20}$$

In general, the bridge frequency $\omega_{b,n}$ is much greater than the driving frequency $n\pi v/L$, especially at lower vehicle velocity. Accordingly, the coefficients $\bar{A}_{4,n}$ and $\bar{A}_{5,n}$ can reduce to

$$\bar{\bar{A}}_{4,n} = (\omega_{b,n})^2 \frac{S_n \Delta_{st,n} \omega_v^2}{2(1 - S_n^2)(\omega_v - \omega_{b,n})(\omega_v + \omega_{b,n})}$$

$$\bar{\bar{A}}_{5,n} = -(\omega_{b,n})^2 \frac{S_n \Delta_{st,n} \omega_v^2}{2(1 - S_n^2)(\omega_v - \omega_{b,n})(\omega_v + \omega_{b,n})}$$
(21,22)

As equation (21) and (22) shown, the two coefficients $\bar{A}_{4,n}$ and $\bar{A}_{5,n}$ are equal in magnitude, but opposite in sign, i.e., $\bar{A}_{4,n} + \bar{A}_{5,n} = 0$. Accordingly, the bridge component response $R_b(t)$ and its Hilbert transform $\hat{R}_b(t)$ can be expressed as

$$R_b(t) = -2\bar{\bar{A}}_{4,n}\sin(\omega_{b,n}t)\sin(\frac{n\pi v}{L}t)$$

$$\hat{R}_b(t) = 2\bar{\bar{A}}_{4,n}\cos(\omega_{b,n}t)\sin(\frac{n\pi v}{L}t)$$
 (23,24)
From the introduce of Hilbert transform aforementioned, the instantaneous amplitude history of

From the introduce of Hilbert transform aforementioned, the instantaneous amplitude history of A(t) can be obtained as

$$A(t) = \sqrt{R_b^2(t) + \hat{R}_b^2(t)} = \left| 2\bar{\bar{A}}_{4,n} \cdot \sin\left(\frac{n\pi v}{L}t\right) \right| = 2\left|\bar{\bar{A}}_{4,n}\right| \cdot \left| \sin\left(\frac{n\pi v}{L}t\right) \right|$$
 (25)

Replacing x with vt in equation (25) yields

$$A\left(\frac{x}{v}\right) = 2\left|\bar{A}_{4,n}\right| \cdot \left|\sin\left(\frac{n\pi x}{L}\right)\right| \tag{26}$$

This equation shows that the instantaneous amplitude history of $A\left(\frac{x}{v}\right)$ of the extracted component response is represented by the mode shape function $\sin\left(\frac{n\pi x}{L}\right)$ of the bridge (in absolute value) multiplied by a constant and time-irreverent coefficient $2\left|\bar{A}_{4,n}\right|$, which is a function of the bridge frequency $\omega_{b,n}$, vehicle frequency ω_v , velocity parameter S_n , and vehicle-induced static deflection $\Delta_{st,n}$ of the beam. It reveals that once the component response corresponding to the certain mode shape of the bridge can be extracted from the response of a passing vehicle when it passed over the bridge, its instantaneous amplitude history is representative of the corresponding mode of the bridge (Yang, Li et al. 2014).

On the other hand, the instantaneous phase $\theta(t)$ can be derived as

$$\theta(t) = \arctan\left(\frac{\hat{R}_b(t)}{R_b(t)}\right) = \arctan(-\cot\omega_{b,n}t) = \omega_{b,n}t - \frac{\pi}{2}$$
 (27)

Herein, it is demonstrated that the bridge frequency can be represented by the slope of instantaneous phase. However, this result has relied on the assumption of that the driving frequency $n\pi v/L$ is much smaller than the bridge frequency. In fact, with the increase of vehicle velocity, the driving frequency cannot be neglected in comparison to the bridge frequency. Therefore, the following section will focus on presenting formula derivation considering this driving frequency.

Set a ratio α of $\bar{A}_{5,n}$ to $\bar{A}_{4,n}$ from equations (17) and (18) and it can be expressed as

$$\alpha = \frac{\bar{A}_{5,n}}{\bar{A}_{4,n}} = -\frac{(1+S_n)^2}{(1-S_n)^2} \cdot \frac{(1-\mu_n^2(1-S_n)^2)}{(1-\mu_n^2(1+S_n)^2)}$$
where μ_n is defined as the ratio of the n-th mode natural frequency of bridge $\omega_{b,n}$ to the vehicle

frequency ω_{ν} ,

$$\mu_n = \frac{\omega_{b,n}}{\omega_v} \tag{29}$$

Then, the component response of
$$R_b$$
 and its Hilbert transform \hat{R}_b can be expressed as
$$R_b = \bar{\bar{A}}_{4,n} \cdot \left[(1 + \alpha) \cos(\omega_{b,n}t) \cos(S_n \omega_{b,n}t) + (1 - \alpha) \sin(\omega_{b,n}t) \sin(S_n \omega_{b,n}t) \right]$$

$$\hat{R}_b = \bar{\bar{A}}_{4,n} \cdot \left[(1 + \alpha) \sin(\omega_{b,n}t) \cos(S_n \omega_{b,n}t) - (1 - \alpha) \cos(\omega_{b,n}t) \sin(S_n \omega_{b,n}t) \right]$$
(30,31)

In this way, the instantaneous phase $\theta(t)$ can be derived as

$$\theta(t) = \arctan\left(\frac{\hat{R}_b(t)}{R_b(t)}\right) = \arctan\left(\frac{\tan(\omega_{b,n}t) - \frac{1-\alpha}{1+\alpha}\tan(S_n\omega_{b,n}t)}{1 + \frac{1-\alpha}{1+\alpha}\tan(S_n\omega_{b,n}t)\tan(\omega_{b,n}t)}\right)$$
(32)

Here assumes a time varying coefficient $\beta(t)$ and make it conten

$$\tan(\beta(t)) = \frac{1-\alpha}{1+\alpha} \tan(S_n \omega_{b,n} t)$$
(33)

Therefore, the instantaneous phase $\theta(t)$ of equation (30) can be expressed as follows

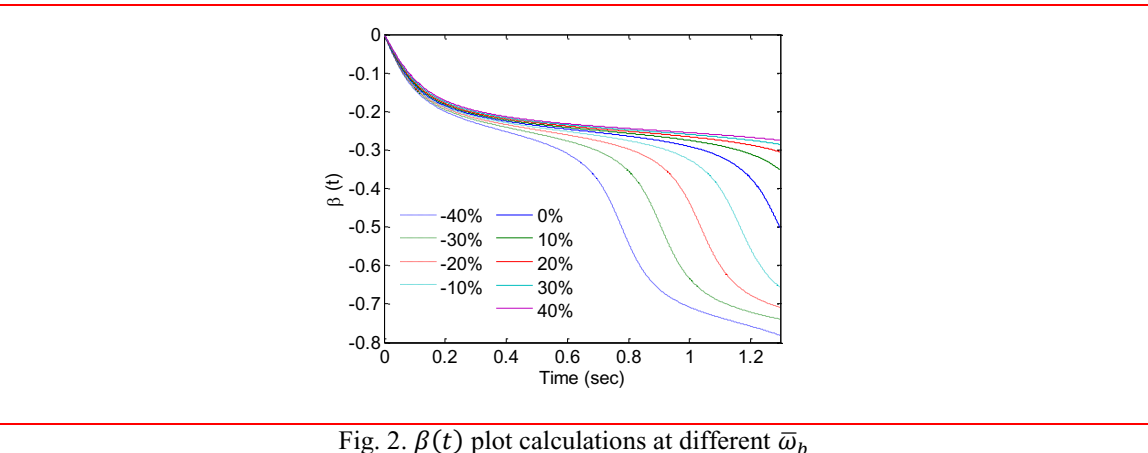
$$\theta(t) = \omega_{b,n}t - \beta(t) \tag{34}$$

Obviously, the equation (34) shows that the slope of the sum of instantaneous phase $\theta(t)$ and $\beta(t)$ represents the bridge frequency. Comparing to the equation (27), it needs to calculate the term of $\beta(t)$, which is related to the vehicle velocity parameter S_n .

Although the proposed HT based approach indicates that the slope of sum $\theta(t) + \beta(t)$ is potential to extract the bridge nature frequencies from a passing vehicle removing vehicle speed effect, it is subject to two main challenges. One is imposed by the requirement of extracted component response R_h associated with single frequency of bridge (n-th mode) from the passing vehicle acceleration history. For this point, it can carry out by feasible signal processing tools, such as singular spectrum and band-pass filters technique, and so on. In this regard, the bridge frequency actually has already been known in signal processing. But this is not contradictory to the present approach for improving extracting bridge frequency. Because this already known bridge frequency

can obtain from applying FFT directly, wavelet analysis approach (Tan, Elhattab et al. 2017) or other ways, which does not remove the effect of the driving frequency and therefore, is considered as a poor identification (marked as $\overline{\omega}_b$ here). This present approach aims to obtain highly accurate identification of a bridge frequency. Although poor identification of bridge frequency can be easily obtained, how to extract R_b from the passing vehicle acceleration is still challengeable. Equation (26) shows that the perfect extracted R_b can obtain results of corresponding the mode shape of the bridge, which can instruct us to extract apposite R_b from the axle responses.

Another challenge is imposed by the calculation of $\beta(t)$, since it is related to the bridge frequencies as shown equation (33). The poor estimated frequency of a bridge $\overline{\omega}_b$ can be used instead. This section will investigate that how much the $\overline{\omega}_b$ influences on $\beta(t)$ as well as the final accuracy of the bridge frequency identification. According to equation (28), assume $\omega_b = 3.86Hz$, $\omega_v = 10.33Hz$ and $S_n = 0.1$; a signal is created by $s(t) = \cos(\omega_b - S_n\omega_b)t + \alpha\cos(\omega_b + S_n\omega_b)t$, where α is calculated based on equation (28). In this case, the total effect time is 1.296s with time steps as 0.002s. Then the HT based approach is applied to extract ω_b from signal s(t). In this processing, $\beta(t)$ is calculated using the given frequency $\overline{\omega}_b$, whose errors varies from -40% to 40% with 10% increment.



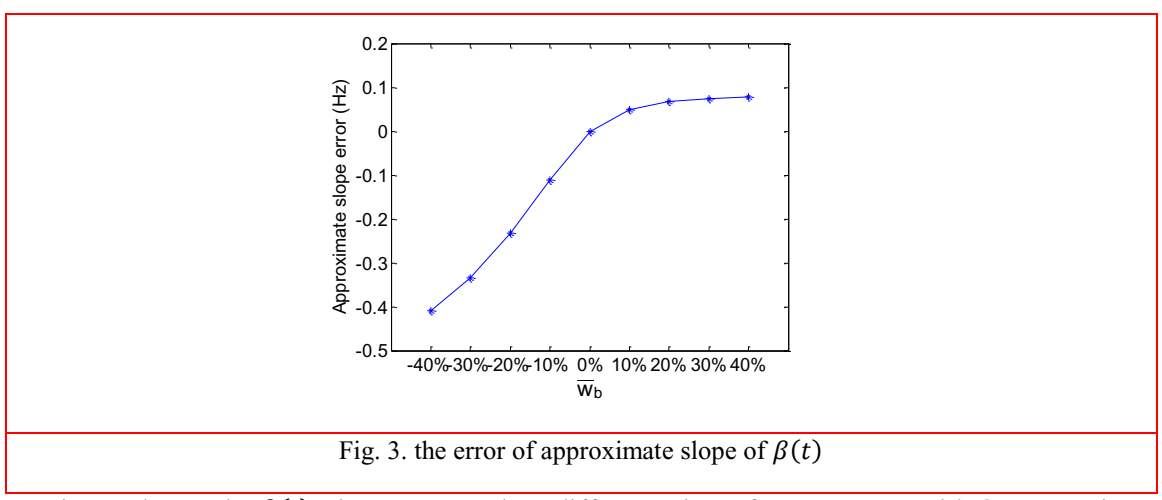
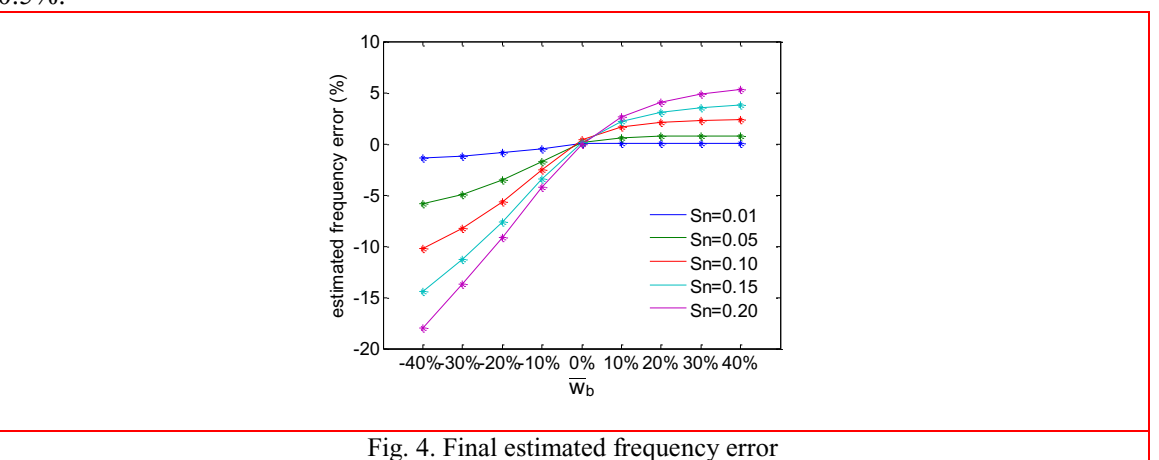
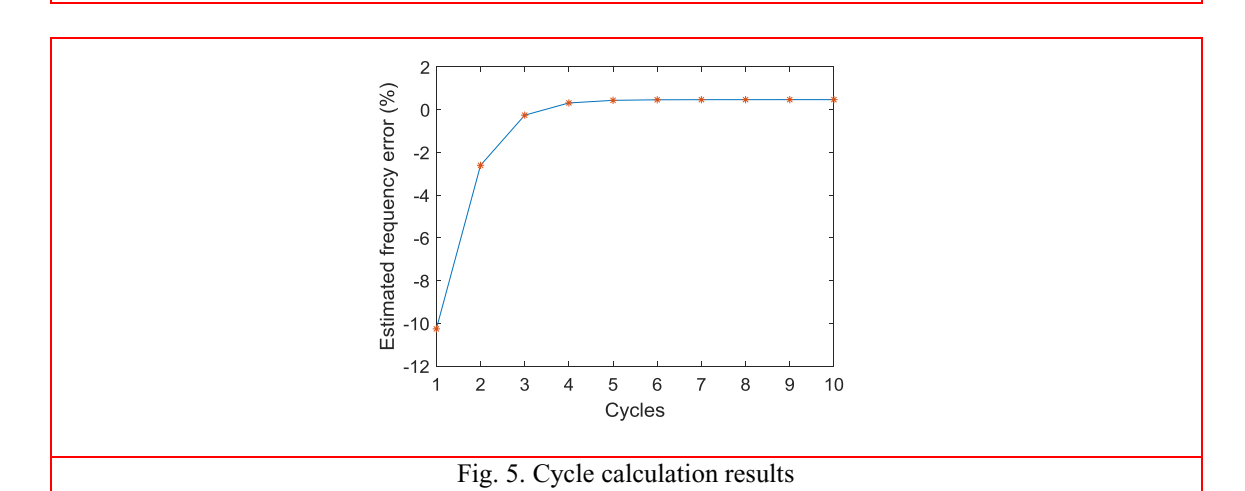


Fig. 2 shows the $\beta(t)$ plots computed at different given frequency $\overline{\omega}_b$ with S_n =0.1. Fig. 3 illustrates the error of approximate slope of these $\beta(t)$ plots comparing to the theoretical one. As it

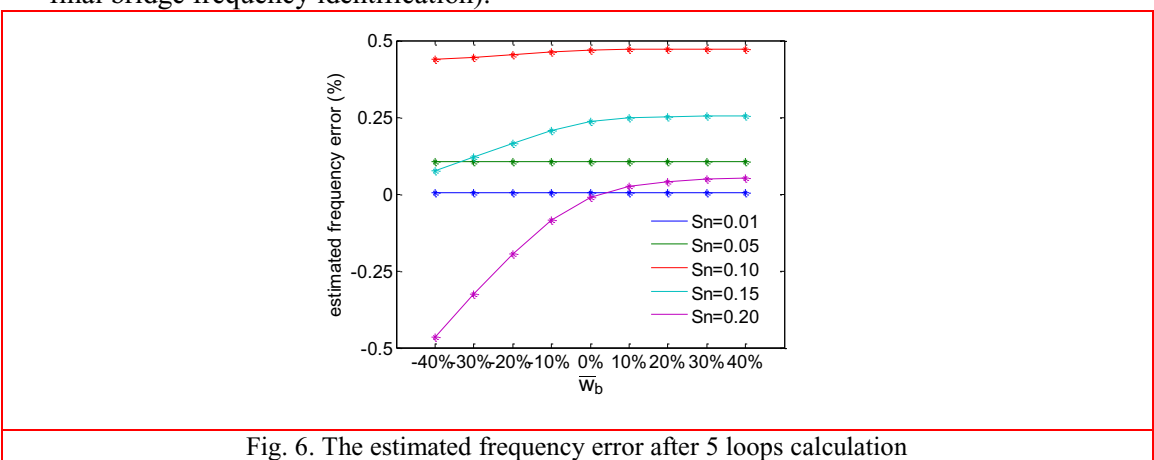
has shown, the lower the given frequency $\overline{\omega}_{\rm h}$, the greater the error result, as well as to the greater $\overline{\omega}_h$, although their errors are obviously lower than the lower given frequency $\overline{\omega}_h$. It is no doubts that these errors of $\beta(t)$ will result in the error to final ω_h identification as well. Fig. 4 shows the error of ω_b identification after applied the proposed HT approach. As expected, the HT based approach apparently and effectively improve the ω_b estimation. To further explain the feasibility of the proposed approach, the results of more cases analysis when $S_n = 0.01, 0.05, 0.15$ and 0.20 are illustrated in Fig. 4 as well. It is worth to notice that the total effect time of signal will be changed corresponding to S_n . For instance, when $S_n = 0.2$, the length of total effect time is changed to 0.648s. From the Fig. 4, the higher S_n will magnify this estimated error, although all of the estimated frequencies have been dramatically improved after applied with the HT based approach in comparison to the given frequency $\overline{\omega}_b$. Practically, the improved estimated frequency can be utilized as a newly given frequency $\overline{\omega}_h$ to recalculate $\beta(t)$ and estimated frequency again and one can repeat these steps until the convergence of $\omega_{\rm h}$. Fig. 5 shows the cycle calculation results in the condition of the first given $\overline{\omega}_b = -40\%~\omega_b$ with S_n =0.1. As it has shown, after enough cycles, the estimated frequency will be convergence and extremely close to theoretical one. Fig. 6 shows all case studies result after five loops' calculation. All of the errors are lower than 0.5%.



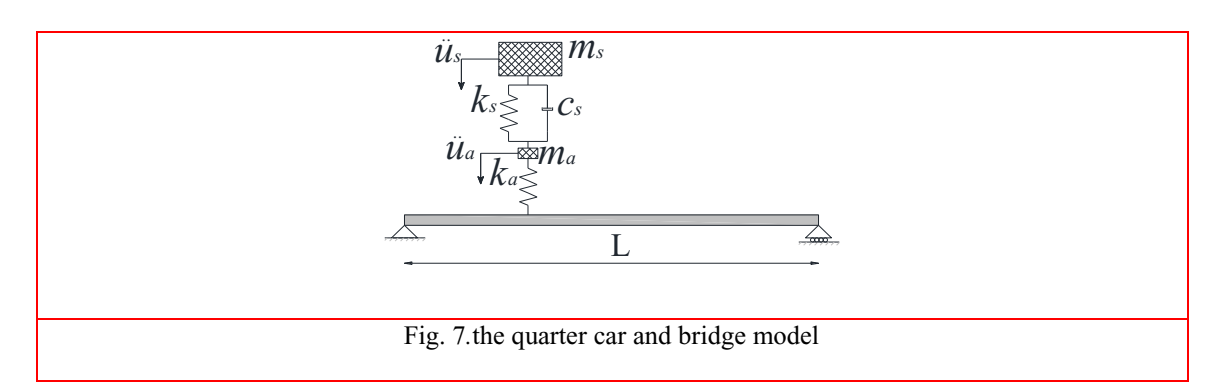


It reaches the conclusion that the calculation of precise $\beta(t)$ is not a challenge anymore conducted by the repeat computation. Once the single component response R_b can be extracted precisely, the bridge frequency can be identified with high accuracy. Therefore, the proposed HT based approach to improve bridge frequency identification of a passing vehicle is summarized as follows:

- (1) Acquisition of the vehicle acceleration responses.
- (2) Obtaining the poor bridge frequencies $\overline{\omega}_b$ applying FFT directly, or wavelet analysis (Tan, Elhattab et al. 2017), etc.
- (3) Extracting a series of single component response R_b at a series of band-pass filters with $\overline{\omega}_b$.
- (4) Calculating instantaneous amplitude history A(t) of HT at each R_b ; simultaneously calculating the MAC (modal assurance criteria) between A(t) and theoretical mode shape of the bridge.
- (5) Choosing the optimum R_b who provides the maximum MAC.
- (6) Calculating the instantaneous phase $\theta(t)$ of HT at the obtained optimum R_b and calculating the time-varying coefficient $\beta(t)$.
- (7) Computing an improved bridge frequency with $\beta(t)$ and $\theta(t)$ and using the improved bridge frequency to calculate the time-varying coefficient $\beta(t)$ again.
- (8) Repeating step (7) until the improved identified frequency convergence (convergence is the final bridge frequency identification).



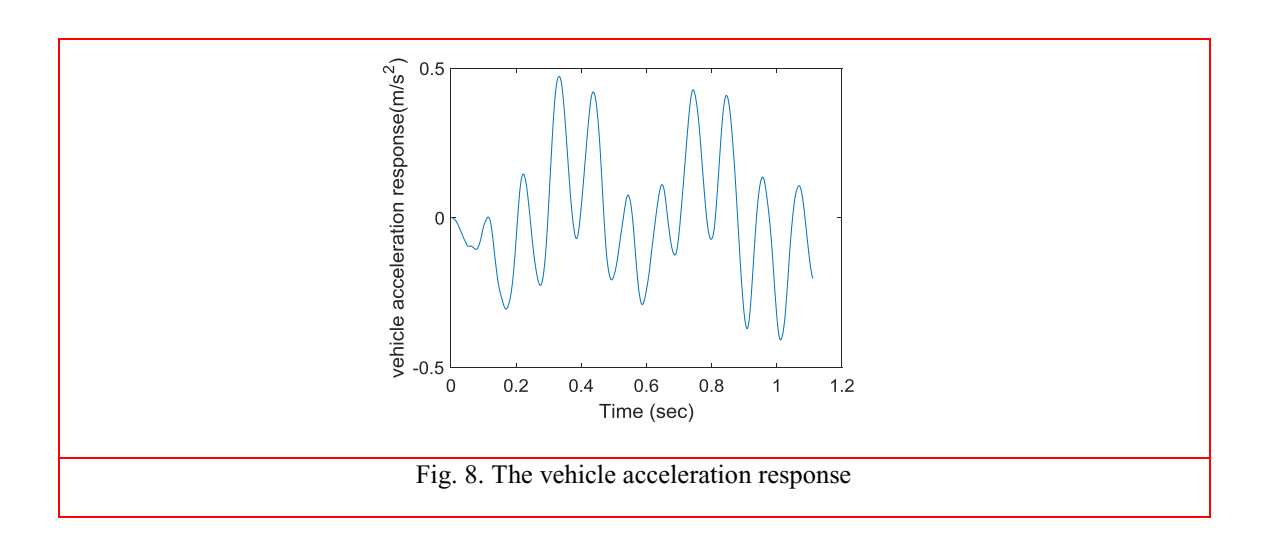
4 Case studies



To verify the feasibility of the proposed approach on improving bridge frequency from a passing vehicle, a quarter-car of VBI model was adopted as shown in Fig. 7. The quarter-car travels with constant speed over the bridge. The vehicle is modeled as a quarter-car model crossing a 50-m approach distance followed by a 20-m simply supported finite element (FE) bridge. The vehicle masses are represented by a sprung mass, m_s, and un-sprung mass, m_a represents the vehicle axle mass and body mass respectively. The Degrees of Freedoms (DOFs) that correspond to the bouncing of the sprung and the axle masses are, u_s, and u_a, respectively. All properties of VBI model is listed in *Table 1* and based upon the work of Cebon (1999). The dynamic interaction between the vehicle and the bridge is implemented in MATLAB (Tan, Elhattab et al. 2017). The road surface profile is not considered in this simulation. Unless otherwise mentioned, the used scanning frequency is 500 Hz. The first two natural frequencies of bridge, *f_b* is 2.171Hz and 8.683Hz respectively. The vehicle frequencies are 0.581Hz and 10.333Hz respectively.

Table 1 Vehicle and bridge properties

Vehicle	properties	Bridge properties					
m_s	14000 kg	Span	20m				
ks	200 kN/m	Density	4800kg/m ³				
c_{s}	10 kN s/m	Width	4 m				
ma	700 kg	Depth	0.8m				
k _a	2750 kN/m	Modulus	$2.75 \times 10^{10} \mathrm{N/m^2}$				



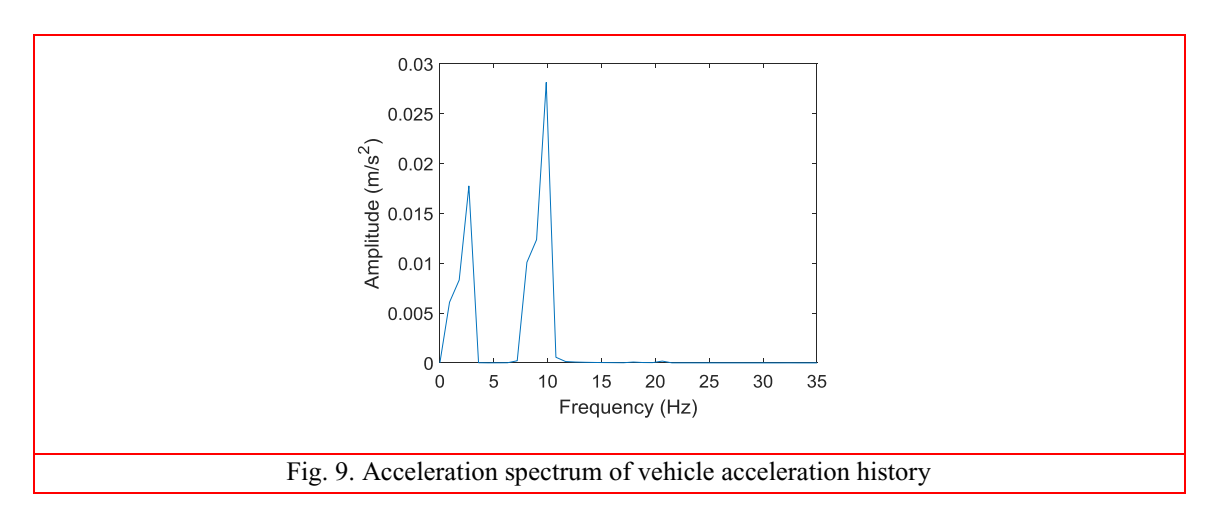
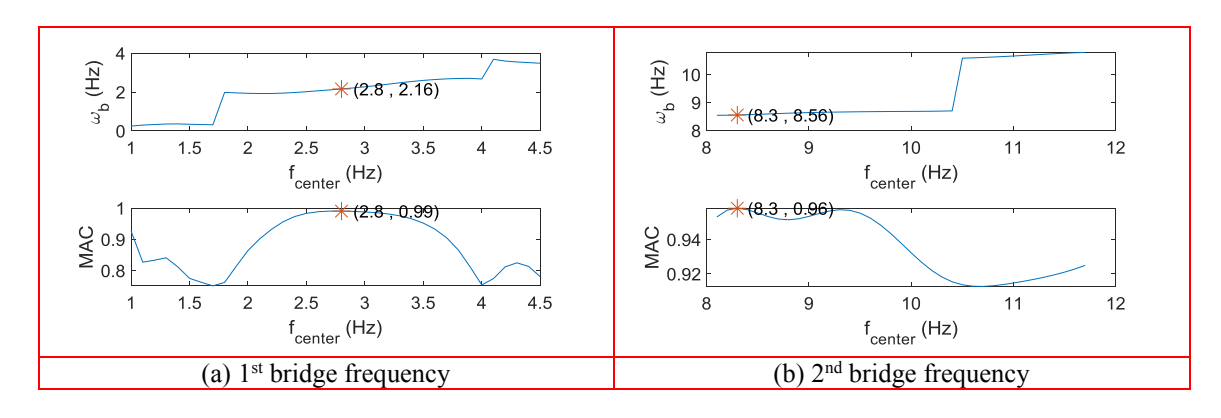


Fig. 8 illustrates the vehicle axle acceleration response for the VBI model mentioned above, where the vehicle velocity is 18m/s. As aforementioned in the analytical theory, this passing vehicle history contains the bridge frequency components. Therefore, the natural frequency of bridge can be extracted after FFT applying to the signal of Fig. 8. Fig. 9 illustrates the spectrum of the recorded response showing two distinctive peaks according to the frequency of 2.693Hz and 9.874Hz respectively, which represents the first two bridge natural frequencies of the bridge, respectively. Since the frequency resolution of FFT is low with short data at the condition of higher vehicle velocity. The spectrum of the test vehicle with FFT cannot point out the precious frequencies of bridges. With the increase in vehicle velocity, the frequency resolution of FFT will be worse. Thus, FFT can only provide a poor frequency identification for short data of the passing vehicle acceleration response. In addition, FFT cannot be used to detect the bridge frequency drop caused by bridge structure damages so as to assess bridge condition. The following section will utilize the proposed HT based approach to improve the extraction of the bridge frequencies.

Generally, the maximum error applying FFT directly will be not greater than 2 times of the theoretical driving frequency (in this case: $f_d = \frac{v}{L} = 0.9 Hz$) because both of the shift frequency and frequency resolution are equal to f_d . For example, in this case, the real first natural bridge frequency should be in the range of $f_{r1} = 2.693 - 2 \times 0.9 = 0.893$; $f_{r2} = 2.693 + 2 \times 0.9 = 4.493$. Then a zero-phase digital 'Butterworth' band-pass filter with a lower order as 6 is applied to the recorded acceleration response to extract the single modal component response. For this band-pass filter, the center frequency f_{center} varies from f_{r1} to f_{r2} , and the two-cut-off frequencies are $f_{c1} = f_{center} - 2 \times f_d$ and $f_{c2} = f_{center} + 2 \times f_d$, respectively.



Therefore, these band-pass filters are applied to extract the first two single component responses R_{b1} and R_{b2} of the bridge, and then these series of extracted R_{b1} and R_{b2} are used to improve the bridge frequency ω_b identification based on the aforementioned procedures. For this case, the results are illustrated in Fig. 10. As it has shown, when the $f_{center} = 2.8Hz$, the corresponding R_{b1} has the maximum MAC and obtains the final $\omega_b = 2.16Hz$, which is extremely close to the theoretical one with regard to the first bridge frequency. Similarly, the 2^{nd} bridge frequency has been improved apparently after applying the proposed approach.

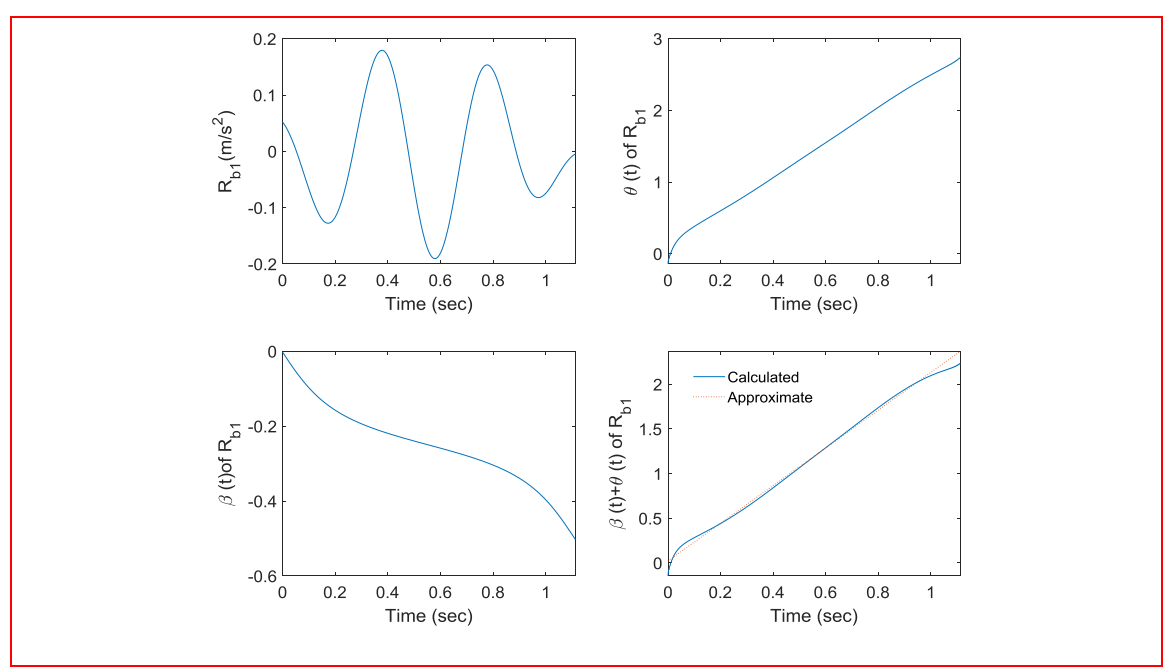


Fig. 11. The improved 1st bridge frequency identification details; top left: single component R_{b1} after bandpass filter; top right: the instantaneous phase $\theta(t)$; bottom left: the time varying coefficient $\beta(t)$; bottom right: $\theta(t)+\beta(t)$

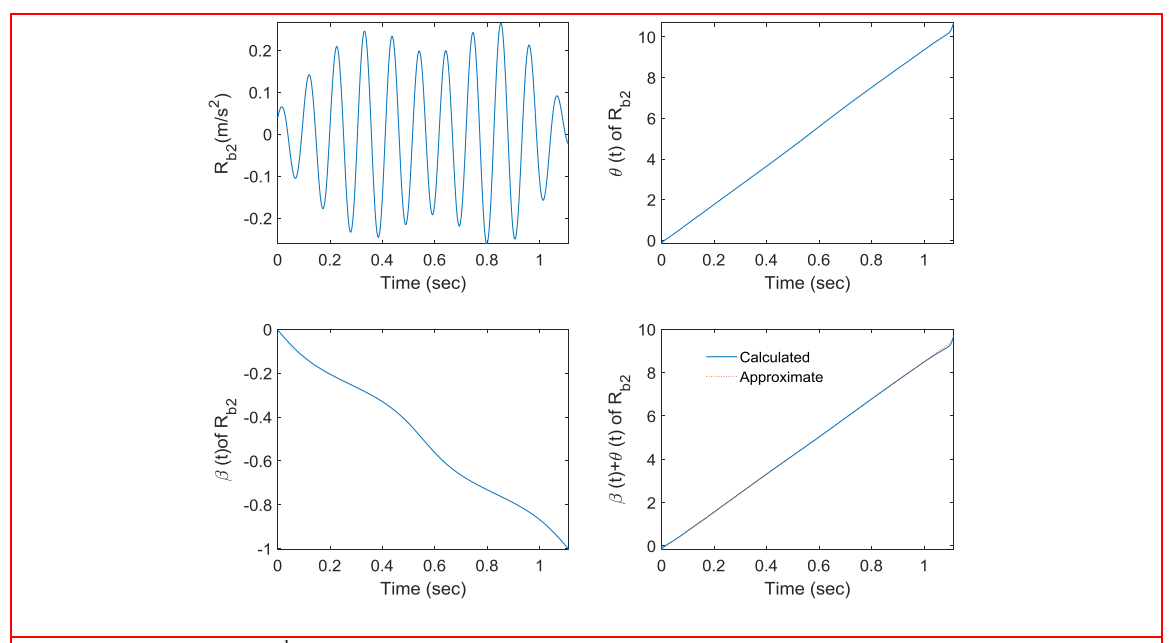


Fig. 12. The improved 2^{nd} bridge frequency identification details; top left: single component R_{b2} after bandpass filter; top right: the instantaneous phase $\theta(t)$; bottom left: the time varying coefficient $\beta(t)$; bottom right: $\theta(t)+\beta(t)$

Fig. 11 and Fig. 12 show the details for improving the bridge frequency ω_b identification based on HT approach. As they have shown, these $\theta(t)$ plots are represented by a nearly straight line and their approximate slopes are calculated as 2.39 and 9.55 respectively. These calculated slopes can be considered as bridge frequencies as equation (27) considering the vehicle velocity parameter effect. However, the errors are great comparing to the theoretical one. Actually, the $\beta(t)$ plots are represented by this vehicle speed effect and clearly, they cannot be ignored directly. From the equation (34), the slopes of plots of $\theta(t) + \beta(t)$ represent the high accuracy identification of bridge frequency removing the effect of vehicle velocity effect and their approximate slopes are calculated as 2.16 and 8.56 respectively.

4.1 Effect of vehicle speed

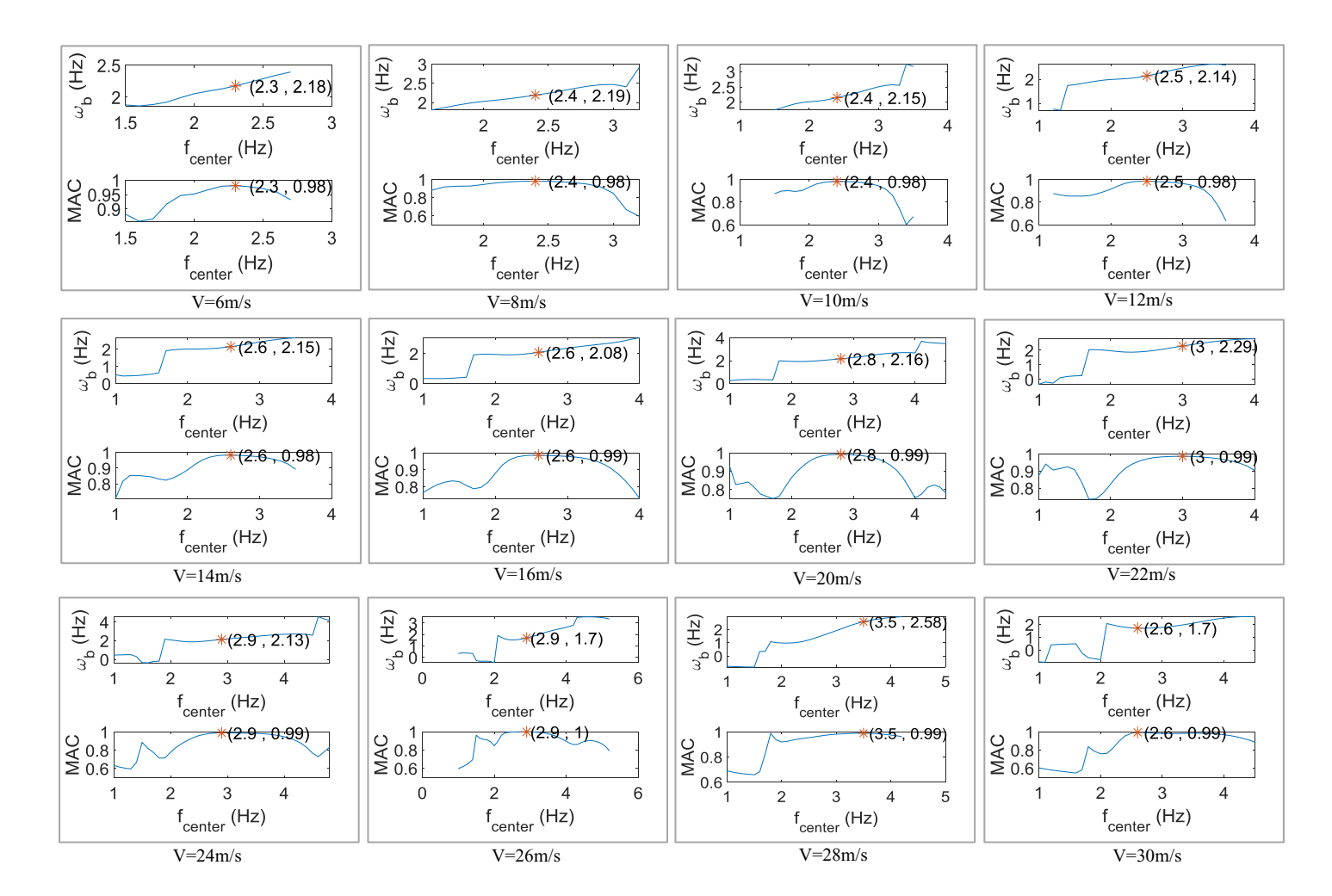


Fig. 13. The improved 1st bridge frequency identification at different vehicle speeds.

In this case, the effect of the vehicle speed on improving the bridge frequency identification is studied for a series of vehicle speeds: v from 6 to 30 m/s with incensement of 2 m/s. Other parameters of VBI remain identical to that studied previously. By following the same procedure, the improved first two bridge frequencies can be extracted from a passing vehicle for each vehicle speed, as shown in Fig. 13 and Fig. 14. Table 2 lists the final bridge frequencies identification values of ω_b and results from HHT directly comparing to theoretical ones.

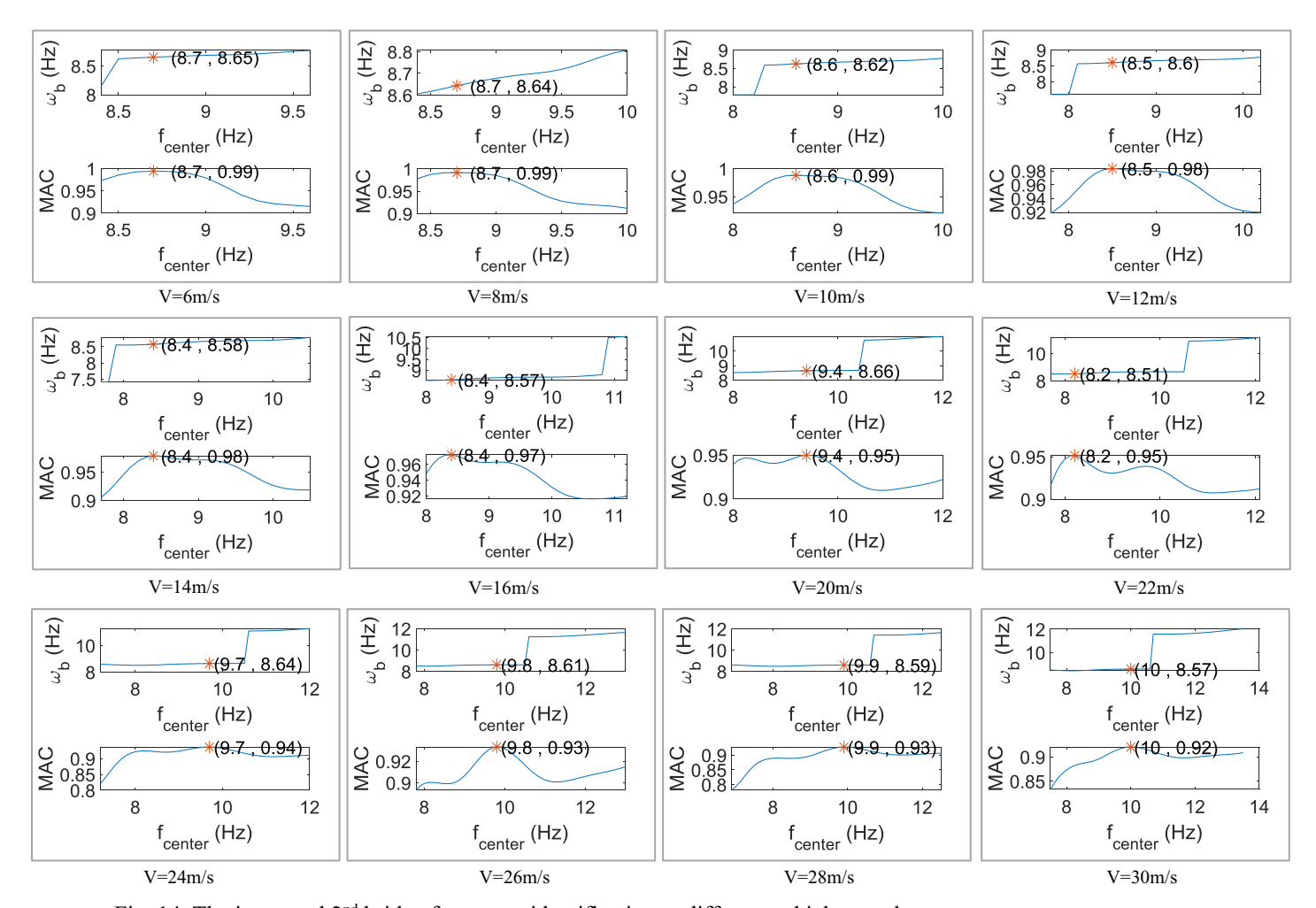


Fig. 14. The improved 2nd bridge frequency identification at different vehicle speeds.

Table 2. The improved bridge frequencies identification results at different vehicle speeds

	locities m/s)	6	8	10	12	14	16	18	20	22	24	26	28	30
	HT (Hz)	2.18	2.19	2.15	2.14	2.15	2.08	2.16	2.29	2.14	2.13	1.70	2.58	1.70
1 st	Error (%)	0.23	1.02	-0.78	-1.48	-0.75	-4.06	-0.48	5.68	-1.40	-1.71	-21.81	18.94	21.46
1 "	FFT (Hz)	2.10	2.40	2.50	2.40	2.09	2.40	2.69	2.00	2.20	2.39	2.59	1.39	1.50
	Error (%)	-3.33	10.48	15.06	10.48	-3.49	10.39	24.06	-8.05	1.25	10.21	19.35	35.84	31.04
	HT (Hz)	8.65	8.64	8.62	8.60	8.58	8.57	8.56	8.66	8.51	8.64	8.61	8.59	8.57
2 ⁿ	Error (%)	-0.34	-0.46	-0.69	-0.91	-1.16	-1.29	-1.45	-0.30	-1.97	-0.49	-0.83	-1.05	-1.30
	FFT (Hz)	8.99	9.19	8.99	8.99	9.08	9.58	9.87	9.98	9.89	9.57	10.36	9.75	10.48

Error	3 57	5 07	2.55	2.57	155	10.20	12.72	14.04	12.00	10.21	10.24	12.20	20.69	ĺ
(%)	3.37	3.87	3.33	3.37	4.55	10.38	13.72	14.94	13.90	10.21	19.34	12.28	20.68	ĺ

In the above processing analysis, all of the poor bridge frequencies identification $\overline{\omega}_b$ are obtained from the FFT spectrum. As it has shown, the $\overline{\omega}_b$ have a greater error at higher vehicle speed. In Table 2, the maximum identification error of FFT is -35.84% for 1st bridge frequency and 20.68% for 2nd bridge frequency. Obviously, the proposed approach has improved the bridge frequencies from a passing vehicle in most the cases. The identification error is less than 1.97% for 2nd bridge frequency. It is observed that when the vehicle speed is not greater than 26 m/s, the results of the improved 1st bridge frequencies are precious and error is less than 5.68%. In contrast, when the vehicle speed is equal to or greater than 26 m/s, the proposed HT based approach is not able to improve the bridge natural frequencies from the poor identification results with FFT.

4.2 Effect of noisy

To further investigate the feasibility of this proposed method, the effect of noisy are investigated. In order to simulate the polluted measurements, white noise is added to the simulated responses of the vehicle. The noisy response is calculated as following formula:

$$\ddot{u}_{noise} = \ddot{u}_{calculated} + E_p N_{oise} \sigma (\ddot{u}_{calculated}) \tag{35}$$

where \ddot{u}_{noise} is the polluted acceleration; E_p is the noise level and N_{oise} is a standard normal distribution vector with zero mean value and unit standard deviation. $\ddot{u}_{calculated}$ is the calculated acceleration, and $\sigma(\ddot{u}_{calculated})$ is their standard deviations.

Table 3. The errors of improved bridge frequencies results at different levels of noisy

	Table 5. The citors of improved bridge nequencies results at different levels of horsy													
Nois leve	•		8	10	12	14	16	18	20	22	24	26	28	30
	0.05	0.22	0.97	-0.73	-1.42	-0.85	-4.02	-1.96	2.67	-1.30	0.00	-24.86	17.31	21.39
	0.1	0.06	1.01	-0.45	-2.06	-0.81	-3.88	-2.31	5.78	0.93	0.34	-24.60	17.45	22.44
1 st	0.15	5.28	0.88	-0.71	-3.61	-0.62	4.68	-0.75	5.89	3.54	0.52	-20.97	16.94	24.04
	0.2	-1.72	0.74	-2.58	-1.55	-2.72	-6.37	-0.53	5.31	-1.22	-4.69	-26.78	63.09	18.72
	0.25	2.75	1.22	-0.64	-3.52	8.87	-6.42	-2.14	5.85	-4.46	-4.35	-25.42	55.91	16.54
	0.05	-0.34	-0.46	-0.69	-0.93	-1.16	-1.28	-1.46	-0.29	-1.97	-0.48	-0.85	-0.94	-1.38
On.	0.1	-0.33	-0.47	-0.69	-0.87	-1.16	-1.32	-1.46	-0.29	-2.00	-0.54	-0.78	-1.17	-1.52
$\frac{2^n}{d}$	0.15	-0.35	-0.45	-0.67	-0.92	-1.17	-1.34	-0.14	-0.24	-2.09	-0.41	-0.89	-1.37	38.81
	0.2	-0.34	-0.48	-0.71	-0.94	-1.09	-1.23	-0.21	0.10	-2.21	-0.42	-0.58	-1.08	38.71
	0.25	-0.31	-0.48	-0.69	-0.95	-1.15	-1.29	-1.45	-0.56	-2.28	-0.32	-0.94	-1.38	38.78

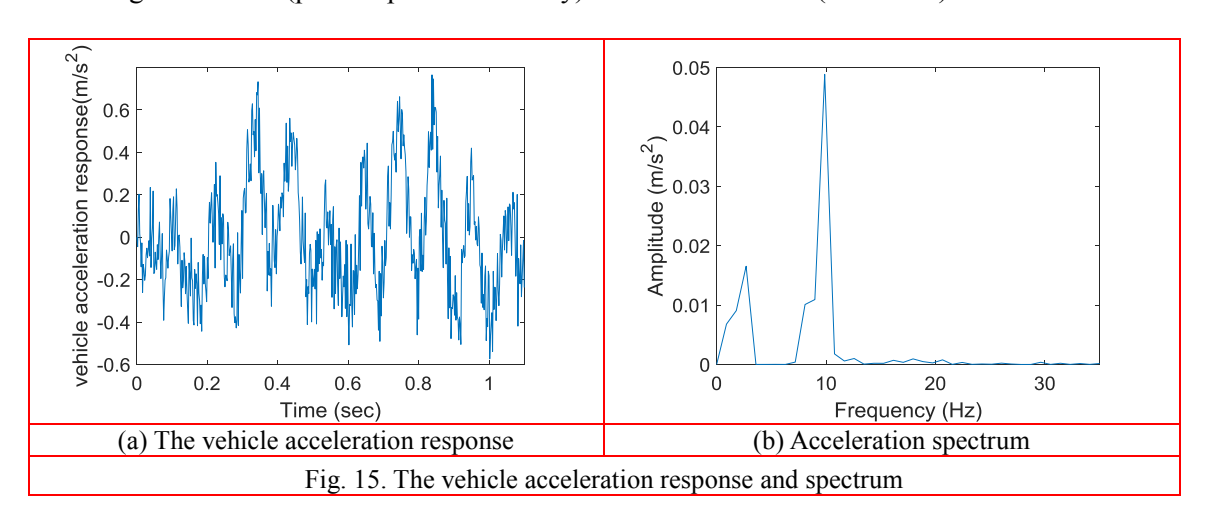
Note: the errors are represented by percentage (%) comparing to theoretical ones.

The different levels of noisy: $E_p = 0.05$, 0.1, 0.15, 0.20 and 0.25 are investigated in this study. By following the same procedure, all the results of the improved bridge frequencies are listed in Table 3. As it has shown, the proposed approach is not sensitive to noisy, possibly because the

procedure of band-pass filtering almost removes the effect of noisy, as long as the FFT can get the generally accurate bridge frequencies $\overline{\omega}_b$. The result of the 2nd bridge frequency is better than that of 1st. The maximum identification error is 8.87% for 1st bridge frequency (except for 26, 28 and 30 m/s) and 2.28% for 2nd bridge frequency (except for 30 m/s).

4.3 Effect of surface roughness

In this case, the effect of road surface roughness is investigated by letting the instrumented vehicle pass over the bridge with rough road profile. The road roughness profile is generated according to the PSD (power spectrum density) curve of "class A" (ISO 1995).



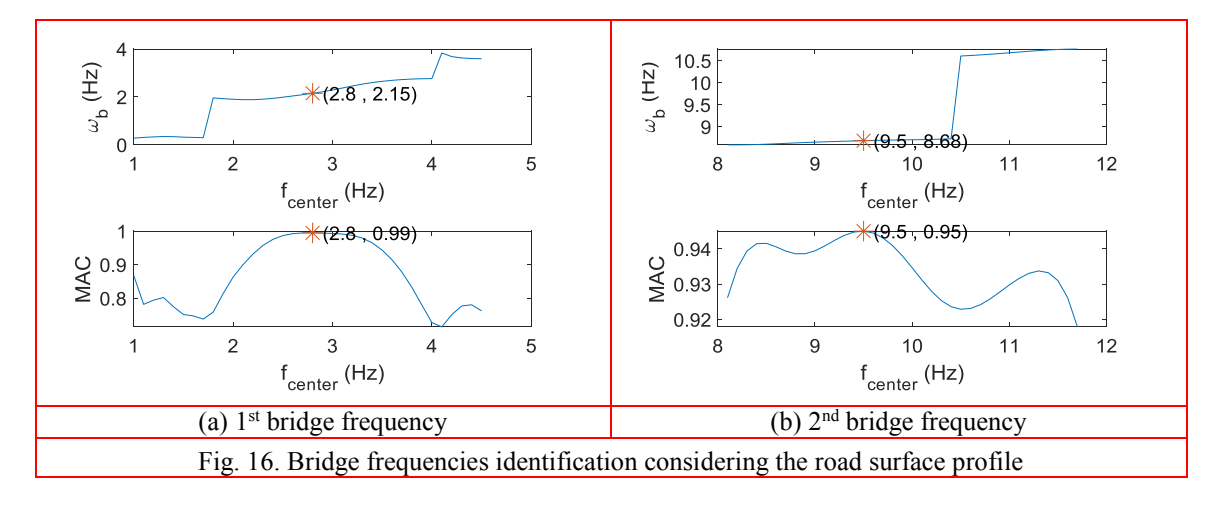


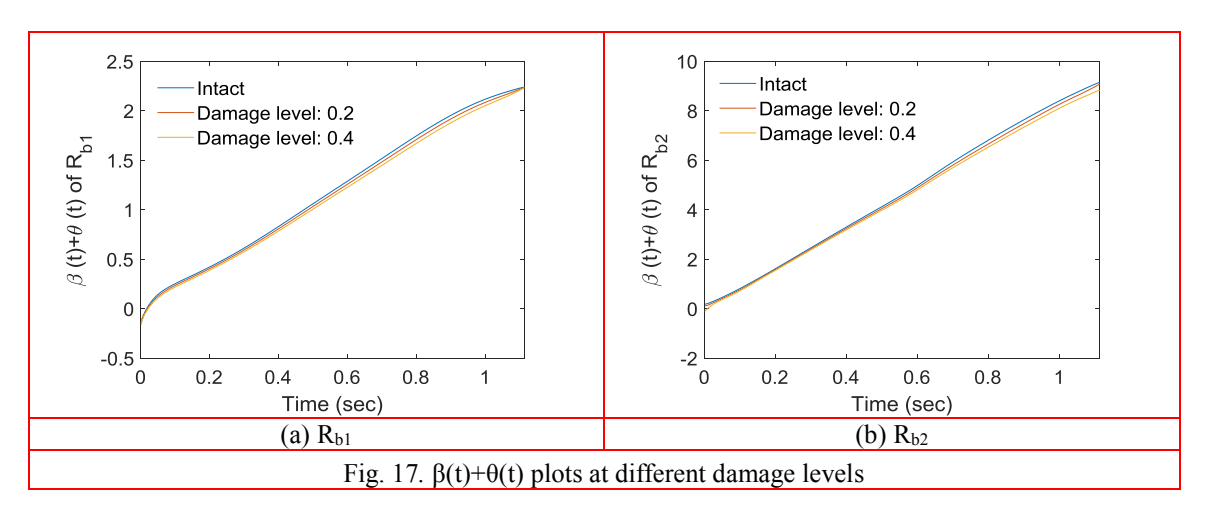
Fig. 15 shows the original crossing vehicle acceleration history at velocity 18 m/s with road roughness and the corresponding frequencies extracted using FFT. As it has shown, at the "class A" road roughness profile, the FFT can still extract the bridge frequency and the first two bridge frequencies are recognized as 2.693Hz and 9.874Hz respectively. Similar to the effect of noise, the following band-pass filtering process can effectively remove the component of response generated by the uneven road surface from the vehicle response. Therefore, the proposed approach can still

improve the bridge frequency. The results are shown in Fig. 16. As expected, it provides the highly precious identification.

5. Estimation bridge condition from a passing vehicle

In this section, the drop in bridge frequency is used as a damage indicator to quantify the damage in the bridge. In this study, bridge damage is simulated using the method proposed by Sinha, Friswell et al. (2002), where the damage is assumed to be extended over a region of three times the beam depth. The element stiffness in this damage region varies from a minimum value at the exact crack location to full stiffness at the edge of the damaged area. The damage level is defined as a ratio of the depth of the crack to the depth of the intact bridge. For example, if the damage level is 0.2 or 20%, it means that the crack depth is 0.16 meters for a 0.8 meters deep bridge.

The FFT method, as mentioned previously, could not be used to accurately identify the bridge frequency at higher speeds. This is due to the low frequency resolution associated with higher vehicle speeds. Therefore, and for the same reason, FFT cannot be used to monitor the shift in the bridge frequency due to structural damages. The frequency step of FFT will not pick up the minor changes happened to the bridge frequency due to structural damages. Therefore, the next section will focus only on using the HT based approach to track the change in the bridge frequency due to the existence of structural damages.



In this case, the damage located at the 0.7L (L=span length) of the bridge. The bridge is modeled three times, one as an intact bridge, and other two cases of different damage levels (e.g. 20% and 40%). By following the procedures mentioned above using the same band-pass filter, Fig. 17 illustrates results of $\beta(t) + \theta(t)$ plots representing the final bridge identification. Herein, all parameters of the VBI model are kept same with the above and the vehicle velocity is 18m/s. As it has shown, there is clear difference of slope in $\beta(t) + \theta(t)$ plots in these three cases. With the increase of damage level, the slope in $\beta(t) + \theta(t)$ plots representing bridge frequency decreases, which can point out the drop of bridge natural frequency due to the structural damage.

In order to investigate the efficacy of the proposed approach in bridge damage detection, different velocities (6m/s, 8m/s, 10m/s, 12m/s and 14m/s) are studied, and the results are illustrated

in Fig. 18 and Fig. 19. In this study, other parameters of VBI remain identical to that studied previously.

As they are shown, with the increment of damage level, the theoretical frequencies of bridge decrease ($f_{TI} > f_{TD1} > f_{TD2}$). Similarly, the identified frequencies of damaged bridge decrease as well ($f_{II} > f_{ID1} > f_{ID2}$). Although the improved bridge frequencies applying HT based approach are not exact to the theoretical ones, the drop of frequencies is clearly found. The error is less than 2.77% for the 1st bridge frequency and 1.16% for the 2nd bridge frequency. It has concluded that the proposed approach is not restricted to frequency resolution, which can be used to quantify the existence of damage using indirect measurements from an inspection vehicle.

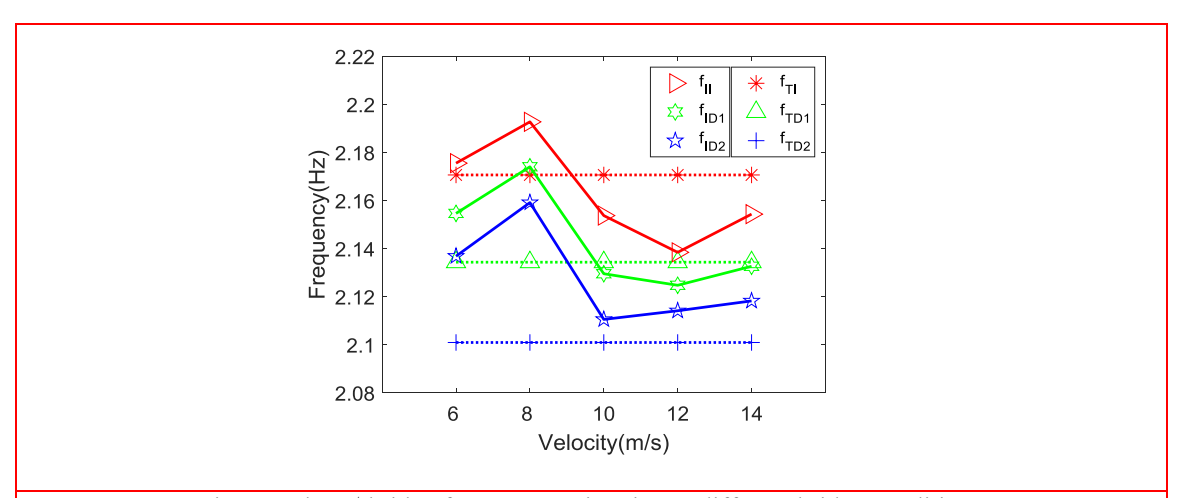


Fig. 18. The 1st bridge frequency estimation at different bridge conditions

*Note: f_{TI} presents the 1st theoretical frequency of the intact bridge, f_{TD1} presents the 1st theoretical frequency of the damaged bridge at level 0.2, f_{TD2} presents the 1st theoretical frequency of the damaged bridge at level 0.4, f_{II} presents the 1st identified frequency of the intact bridge, f_{ID1} presents the 1st identified frequency of the damaged bridge at level 0.2, fID2 presents the 1st identified frequency of the damaged bridge at level 0.4.

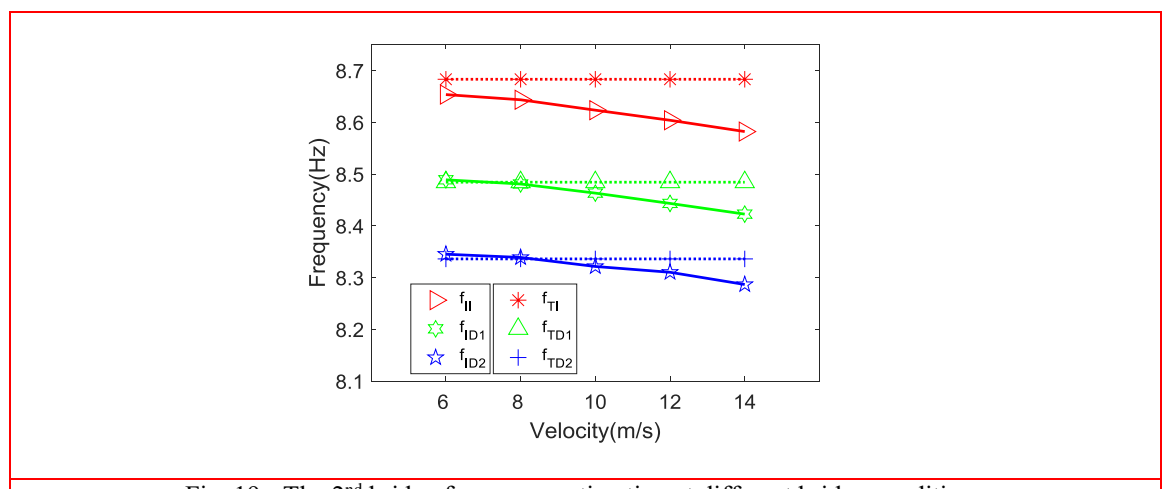


Fig. 19. The 2nd bridge frequency estimation at different bridge conditions

* Note: f_{TI} presents the 2^{nd} theoretical frequency of the intact bridge, f_{TD1} presents the 2^{nd} theoretical frequency of the damaged bridge at level 0.2, f_{TD2} presents the 2^{nd} theoretical frequency of the damaged

bridge at level 0.4, f_{II} presents the 2nd identified frequency of the intact bridge, f_{ID1} presents the 2nd identified frequency of the damaged bridge at level 0.2, fID2 presents the 2nd identified frequency of the damaged bridge at level 0.4.

Conclusions

This paper introduces a new approach combined with HT and band-pass filter technique to improve the bridge natural frequency identification from a passing vehicle. A closed-form solution associated with the bridge frequency removing the effect of vehicle velocity is derived from a passing vehicle response. To implement the proposed approach, a rough bridge frequency is known in advance, which can be achieved by FFT directly. Since FFT is restricted to the frequency resolution as well as the effect of vehicle velocity, the identified frequency accuracy is low. The proposed approach is applied to improve the bridge frequency from a passing vehicle.

In this approach, the most important procedure is to extract the perfect single modal component response from a vehicle response. It has demonstrated that as long as the single modal component response is achieved well enough, the slop of $\beta(t) + \theta(t)$ can give the extremely high-precious improved bridge frequency identification by the loop calculation. In this paper, it obtains the appropriate single modal component response R_b who reaches the maximum MAC of instantaneous amplitude history A(t) with HT from a series of band-pass filters. Followed by this way, the HT based approach has effectively and clearly improved the bridge frequency extraction. The improved identification error is less than 1.97% for the 2^{nd} bridge frequency, and 5.68% for the 1^{st} bridge frequencies (vehicle speed is not greater than 26 m/s).

This study investigates the approach feasibility on the effect of noisy and road surface roughness. It has concluded that because of the procedure of band-pass filtering, the proposed approach is not sensitive to the noise and road surface roughness, as long as the FFT can still achieve the rough bridge frequency from the response of the vehicle. In addition, the proposed approach is not restricted to the frequency resolution. The improved bridge frequencies represented by the slope of $\beta(t) + \theta(t)$ can point out the drop of frequency as the damage extent increases. Therefore, the approach has strong potential to provide a quick estimation of the bridge health condition.

Acknowledgment

This research is sponsored by National Science of Foundation (NSF-CNS-1645863). Any opinions, findings, and conclusions or recommendations expressed in this publication are those of the authors and do not necessarily reflect the view of the sponsors.

References

Carden, E. P. (2004). "Vibration Based Condition Monitoring: A Review." <u>Structural Health Monitoring</u> **3**(4): 355-377.

Cebon, D. (1999). Handbook of vehicle-road interaction, ALWAYS

Chupanit, P. and C. Phromsorn (2012). "The importance of bridge health monitoring." <u>International Science Index</u> **6**: 135-138.

Cunha, A., et al. "An indirect bridge inspection method incorporating a wavelet-based damage indicator and pattern recognition."

- González, A., et al. (2012). "Identification of damping in a bridge using a moving instrumented vehicle." <u>Journal of Sound and Vibration</u> **331**(18): 4115-4131.
- Hester, D. and A. González (2012). "A wavelet-based damage detection algorithm based on bridge acceleration response to a vehicle." <u>Mechanical Systems and Signal Processing</u> **28**: 145-166.
- Huang, N. E. (2014). "Hilbert–Huang Transform and Its Applications." 16.
- ISO, I. (1995). Mechanical vibration-Road surface profiles-Reporting of measured data, International Organization for Standardization (ISO) Geneva.
- Keenahan, J., et al. (2013). "The use of a dynamic truck-trailer drive-by system to monitor bridge damping." <u>Structural Health Monitoring</u> **13**(2): 143-157.
- Khorram, A., et al. (2012). "Comparison studies between two wavelet based crack detection methods of a beam subjected to a moving load." <u>International Journal of Engineering Science</u> **51**: 204-215.
- Lin, C. W. and Y. B. Yang (2005). "Use of a passing vehicle to scan the fundamental bridge frequencies: An experimental verification." Engineering Structures **27**(13): 1865-1878.
- Mahato, S., et al. (2017). "Combined wavelet–Hilbert transform-based modal identification of road bridge using vehicular excitation." <u>Journal of Civil Structural Health Monitoring</u> 7(1): 29-44.
- Malekjafarian, A., et al. (2015). "A Review of Indirect Bridge Monitoring Using Passing Vehicles." Shock and Vibration **2015**: 1-16.
- Malekjafarian, A. and E. J. Obrien (2014). "Identification of bridge mode shapes using Short Time Frequency Domain Decomposition of the responses measured in a passing vehicle." <u>Engineering Structures</u> **81**: 386-397.
- Malekjafarian, A. and E. J. Obrien (2017). "On the use of a passing vehicle for the estimation of bridge mode shapes." <u>Journal of Sound and Vibration</u> **397**: 77-91.
- McGetrick, P. J. and C. W. Kim (2013). "A Parametric Study of a Drive by Bridge Inspection System Based on the Morlet Wavelet." <u>Key Engineering Materials</u> **569-570**: 262-269.
- Nguyen, K. V. and H. T. Tran (2010). "Multi-cracks detection of a beam-like structure based on the on-vehicle vibration signal and wavelet analysis." <u>Journal of Sound and Vibration</u> **329**(21): 4455-4465.
- Obrien, E. J. and A. Malekjafarian (2016). "A mode shape-based damage detection approach using laser measurement from a vehicle crossing a simply supported bridge." <u>Structural Control and Health Monitoring</u> **23**(10): 1273-1286.
- Obrien, E. J., et al. (2017). "Application of empirical mode decomposition to drive-by bridge damage detection." <u>European Journal of Mechanics A/Solids</u> **61**: 151-163.
- Oshima, Y., et al. (2014). "Damage assessment of a bridge based on mode shapes estimated by responses of passing vehicles." <u>Smart Structures and Systems</u> **13**(5): 731-753.
- Sinha, J. K., et al. (2002). "Simplified Models for the Location of Cracks in Beam Structures Using Measured Vibration Data." Journal of Sound and Vibration **251**(1): 13-38.
- Tan, C., et al. (2017). ""Drive-by" bridge frequency-based monitoring utilizing wavelet transform." Journal of Civil Structural Health Monitoring.
- Tan, C., et al. (2017). <u>Wavelet Based Damage Assessment and Localization for Bridge Structures</u>. 26th ASNT Research Symposium.
- Yang, Y. and C. Lin (2005). "Vehicle-bridge interaction dynamics and potential applications." Journal of Sound and Vibration **284**(1): 205-226.
- Yang, Y. B. and K. C. Chang (2009). "Extracting the bridge frequencies indirectly from a passing vehicle: Parametric study." Engineering Structures **31**(10): 2448-2459.
- Yang, Y. B. and K. C. Chang (2009). "Extraction of bridge frequencies from the dynamic response of a passing vehicle enhanced by the EMD technique." <u>Journal of Sound and Vibration</u> **322**(4-5): 718-739.

- Yang, Y. B., et al. (2014). "Constructing the mode shapes of a bridge from a passing vehicle: a theoretical study." <u>Smart Structures and Systems</u> **13**(5): 797-819.
- Zhang, Y., et al. (2012). "Damage detection by mode shape squares extracted from a passing vehicle." <u>Journal of Sound and Vibration</u> **331**(2): 291-307.